

# Transient Excitation of a Straight Thin-Wire Segment: a New Look at an Old Problem

Anton G. Tijhuis, *Member, IEEE*, Peng Zhongqiu, and Amelia Rubio Bretones

**Abstract**—The transient excitation of a straight thin-wire segment is analyzed with the aid of a one-dimensional integral equation for the current along the wire. A new almost exact derivation of that equation is given, in which only the radial current on the end faces is approximated. The integral equation obtained turns out to be identical to the “reduced” version of Pocklington’s equation. Based on this derivation, existing and new numerical solution techniques are critically reviewed. Pocklington’s equation and Hallén’s equivalent form are solved directly by marching on in time as well as indirectly via a transformation to the frequency domain. In the frequency-domain implementation, a fixed coarse space discretization is used for all relevant frequencies. For Pocklington’s equation, a conventional moment-method discretization leads to a Toeplitz matrix that is inverted with Levinson’s algorithm. For Hallén’s equation, the Toeplitz structure is disturbed, and the frequency-domain constituents are determined with the aid of the conjugate-gradient-FFT method. To this end, initial estimates are generated by marching on in frequency and using a new extrapolation scheme. Illustrative numerical results are presented and discussed.

## I. INTRODUCTION

ALMOST a century has passed since Pocklington first formulated his integral equation for the total current along a straight thin-wire segment embedded in a homogeneous lossless dielectric [1]. There, Pocklington also presented an approximate solution to his equation. Since then, both the formulation and the solution of the thin-wire integral equation have been the subject of continuous investigation by many researchers.

The most important development in the formulation was due to Hallén [2], [3], who derived an equivalent equation that can be used to determine the unknown current iteratively. The first iteration step can be carried out in closed form, and produces a correction to Pocklington’s result. Hallén’s procedure was applied and/or improved by several authors [4]–[7]. More recent studies are concerned with the uniqueness of the solution, with the

well-posedness of both Pocklington’s and Hallén’s equation, and with the choice between using an exact or a reduced kernel in the formulation [8], [9].

From a numerical point of view, the excitation of a straight thin-wire segment is regarded as a standard canonical problem. Perhaps, this can be explained from the fact that accurate closed-form expressions for the current distribution were available at an early stage. Further, the configuration itself is of practical interest in antenna design and in wire-grid modeling. Almost any existing solution technique in electromagnetics has been tested for a thin-wire geometry. A notable example is the method of moments, which was applied for harmonic time variation in [10]–[14], and for arbitrary time variation in [15]–[19]. The natural oscillations of the configuration were employed in the so-called singularity expansion method [20], [21]. In [22], the identification problem was investigated by reconstructing the natural frequencies of a thin wire from the known transient response. The most recent addition consists of different versions of the conjugate-gradient method [23]–[27].

In the present paper, we formulate the thin-wire integral equation with the aid of modern integral-representation theory as presented in [28] and applied in [29]. The starting point is a three-dimensional field representation that relates the total electric field at an arbitrary observation point to the surface current on a perfectly conducting obstacle. First, it is shown how this representation is used in the classical derivation of the so-called reduced and exact forms of Pocklington’s equation. Second, by considering this representation with the observation point on the central axis of the cylinder, a new almost exact derivation of the thin-wire integral equation is given. The only approximation involved is that of the radial current on the end faces. This quantity is estimated independently with the aid of Maxwell’s equations. Surprisingly, the integral equation obtained is identical to the reduced version of Pocklington’s equation.

Next, we review a number of numerical techniques for solving this equation and the form derived by Hallén. We determine the space-time behavior of the unknown current directly in the time domain and indirectly, via a transformation to the frequency domain. In the time-domain procedures, we discretize the integral equation in space and time, and we solve the resulting system of linear equations recursively in discretized time. This procedure is known as the marching-on-in-time method. We

Manuscript received January 31, 1991; revised August 5, 1992. The work of P. Zhongqiu was supported by the State Education Commission of China. The work of A. R. Bretones was supported by the Dirección General de Investigación Científica y Técnica, Spain.

A. G. Tijhuis is with the Laboratory of Electromagnetic Research, Department of Electrical Engineering, Delft University of Technology, 2600 GA Delft, The Netherlands.

P. Zhongqiu is with the Department of Electromagnetic Field Engineering, University of Electronic Science and Technology of China, 610054 Chengdu, Sichuan, China.

A. Rubio Bretones is with the Departamento de Física Aplicada, Facultad de Ciencias, Universidad de Granada, 18071 Granada, Spain.  
IEEE Log Number 9204928.

discuss the accepted implementation for Pocklington's equation [16], [19], and develop a new one for Hallén's equation.

In our frequency-domain solution, we follow the idea explained in [30], and choose a fixed space discretization for all frequencies. The mesh size in this discretization is much larger than the one used in "conventional" frequency-domain computations. For Pocklington's equation, we discretize the transformed integral equation by the simplest form of the procedure proposed in [13]. The resulting Toeplitz system of linear equations for the discretized current is solved by Levinson's algorithm. For Hallén's equation, we follow the suggestion of [30] more closely, and transform the space-discretized time-domain integral equation. The system of linear equations thus obtained does not have a Toeplitz structure, but it can be solved with the aid of the conjugate-gradient FFT method [25]–[27]. We improve the efficiency of this method by exploiting the feature that, for a fixed discretization, the discretized current varies continuously with frequency. Therefore, we can generate successive initial estimates by marching on in frequency and using a new extrapolation scheme.

In view of space limitations, we concentrate on formulating the relevant integral equations and on analyzing the numerical methods that we have employed to solve them. As an illustration, a few simple numerical results are presented for a single wire geometry. More extensive discussions of such results can be found elsewhere.

## II. FORMULATION OF THE PROBLEM

A perfectly conducting, straight thin-wire segment of length  $L$  with a circular cross section of radius  $a$  is embedded in a homogeneous, lossless dielectric with permittivity  $\epsilon$  and permeability  $\mu$ . As depicted in Fig. 1, the interior of the wire is denoted by  $\mathcal{D}$ , the boundary by  $\partial\mathcal{D}$ , and the exterior by  $\bar{\mathcal{D}}$ . On  $\partial\mathcal{D}$ , a piecewise-continuous unit normal vector  $\mathbf{n}(\mathbf{r})$  is pointing into  $\bar{\mathcal{D}}$ . A cylindrical Cartesian coordinate system is introduced with the central axis of the wire located at  $\{\mathbf{r} = z\mathbf{i}_z | 0 < z < L\}$  and with  $\boldsymbol{\rho}$  as the position vector in the plane perpendicular to the  $z$ -axis, i.e.,  $\mathbf{r} = z\mathbf{i}_z + \boldsymbol{\rho}$  and  $\boldsymbol{\rho} = \rho\mathbf{i}_\rho(\phi)$ . The wire is excited by an incident electromagnetic field  $\{\mathcal{E}^i(\mathbf{r}, t), \mathcal{H}^i(\mathbf{r}, t)\}$ , which is a solution of Maxwell's equation in absence of the wire, and/or driven by an impressed voltage  $\mathcal{V}(t)$  across the gap  $z_g - \delta < z < z_g + \delta$ . The dimensions of the wire satisfy the inequalities  $\delta \ll a \ll L$ . Both the incident field on  $\partial\mathcal{D}$  and the impressed voltage are identically zero before the initial instant  $t = t_0$ . The aim of the computation is to determine the total current  $I(z, t)$  flowing through the wire and, subsequently, the electromagnetic field surrounding it.

### A. Integral Relation for the Electric Field

The principal tool in the theoretical description of the problem outlined above is a one-dimensional space-time integro-differential equation for  $I(z, t)$ . The most suitable starting point for deriving such an equation is the integral

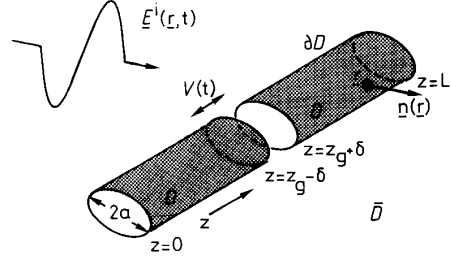


Fig. 1. Transient excitation of a straight thin-wire segment by an incident field or an impressed voltage.

relation for the electric field

$$\left\{0, \frac{1}{2}, 1\right\} \epsilon \partial_t \mathcal{E}(\mathbf{r}, t) - \epsilon \partial_t \mathcal{E}^i(\mathbf{r}, t) = \nabla \nabla \cdot \mathcal{A}(\mathbf{r}, t) - \frac{1}{c^2} \partial_t^2 \mathcal{A}(\mathbf{r}, t) \quad (1)$$

which holds for all  $t$  and for  $\mathbf{r} \in \{\mathcal{D}, \partial\mathcal{D}, \bar{\mathcal{D}}\}$ . For  $\mathbf{r} \in \partial\mathcal{D}$ , the representation (1) pertains to the limiting value of  $\mathcal{E}(\mathbf{r}, t)$  upon approaching  $\partial\mathcal{D}$  from  $\bar{\mathcal{D}}$ . In (1), the wave speed  $c$  is given by  $c \stackrel{\text{def}}{=} 1/\sqrt{\epsilon\mu}$ , and  $\mathcal{A}(\mathbf{r}, t)$  is the magnetic vector potential

$$\mathcal{A}(\mathbf{r}, t) \stackrel{\text{def}}{=} \oint_{\partial\mathcal{D}} \frac{\mathcal{J}(\mathbf{r}', t - R/c)}{4\pi R} dS(\mathbf{r}') \quad (2)$$

with  $R \stackrel{\text{def}}{=} |\mathbf{r} - \mathbf{r}'|$ , and with

$$\mathcal{J}(\mathbf{r}, t) \stackrel{\text{def}}{=} \mathbf{n}(\mathbf{r}) \times \mathcal{H}(\mathbf{r}, t) \quad (3)$$

being the electric surface-current density induced on  $\partial\mathcal{D}$ . The integral relation (1) follows directly by subjecting the differential form of Maxwell's equations to a spatial Fourier transformation over either  $\mathcal{D}$  or  $\bar{\mathcal{D}}$ , and to a temporal Laplace transformation. For details about this derivation, the reader is referred to [28] or [29].

In principle, the integral relation (1) provides a complete mathematical description of the problem. However, this description is not suitable for describing the field in a narrow gap. For that field, an alternative formulation is needed. Since the end faces on both sides of the gap are electrically impenetrable, we have

$$\mathcal{E}_{\rho,\phi}([z_g \pm \delta]\mathbf{i}_z + \boldsymbol{\rho}, t) = 0 \quad (4)$$

for  $\rho \stackrel{\text{def}}{=} |\boldsymbol{\rho}| \leq a$ . Using the features that  $\mathcal{E}(\mathbf{r}, t)$  is continuous in  $z$  and that  $\delta \ll a$ , we may therefore neglect the transverse components  $\mathcal{E}_{\rho,\phi}$  throughout the gap. Thus, we have in good approximation

$$\mathcal{E}(z\mathbf{i}_z + \boldsymbol{\rho}, t) \approx \mathcal{E}_z(z\mathbf{i}_z + \boldsymbol{\rho}, t)\mathbf{i}_z \quad (5)$$

for  $z_g - \delta < z < z_g + \delta$  and  $0 \leq \rho \leq a$ , with

$$\int_{z_g - \delta}^{z_g + \delta} \mathcal{E}_z(z\mathbf{i}_z + \boldsymbol{\rho}, t) dz = -\mathcal{V}(t) \quad (6)$$

for  $0 \leq \rho \leq a$ .

As  $\delta \downarrow 0$ , (1)–(3), (5) and (6) determine the surface current excited on the wire. To arrive at the pertinent integral equation, the following steps are required.

- Consider the integral relation (1) for  $\mathbf{r} \in \partial\mathcal{D}$ , take the vector product with  $\mathbf{n}(\mathbf{r})$ , and use the boundary condition  $\mathbf{n}(\mathbf{r}) \times \mathcal{E}(\mathbf{r}, t) = \mathbf{0}$ .

- Consider the integral relation (1) for  $\mathbf{r} \in \bar{\mathcal{D}}$ , locate  $\mathbf{r}$  just inside the gap region, and take the vector product with  $\mathbf{n}(\mathbf{r}) = \mathbf{i}_\rho$ .

- Use the definition (3) for  $\mathcal{I}(\mathbf{r}, t)$  and the continuity of  $\mathcal{I}(\mathbf{r}, t)$  to eliminate the contributions of the end faces adjoining the gap.

- Take the limit for  $\delta \downarrow 0$  and use (5) and (6).

Carrying out these steps results in the boundary integral equation

$$\begin{aligned} [\mathbf{n}(\mathbf{r}) \times \nabla] \nabla \times \mathcal{I}(\mathbf{r}, t) - \frac{1}{c^2} \mathbf{n}(\mathbf{r}) \times \partial_t^2 \mathcal{I}(\mathbf{r}, t) \\ = \epsilon \partial_t \mathcal{I}'(t) \delta(z - z_g) \mathbf{i}_\phi - \epsilon \mathbf{n}(\mathbf{r}) \times \partial_t \mathcal{E}^i(\mathbf{r}, t) \quad (7) \end{aligned}$$

which holds for  $\mathbf{r} \in \partial\mathcal{D}$  and  $t_0 \leq t < \infty$ . In (7),  $\delta(z)$  denotes Dirac's delta distribution. The boundary  $\partial\mathcal{D}$  is now considered to enclose the gap region as well. Equation (7) is nothing but the well-known electric-field integral equation (EFIE) for scattering by a perfectly conducting obstacle. In that context, the voltage term on the right-hand side may be regarded as originating from an equivalent incident field.

In principle, this completes the formulation of the problem. However, the information that  $a \ll L$  can be used to arrive at a simpler one-dimensional formulation. In the upcoming subsections, several steps are reviewed that lead to this goal. In all cases, this leads to an integro-differential equation for the total current

$$\mathcal{I}(z, t) \stackrel{\text{def}}{=} a \int_{-\pi}^{\pi} \mathcal{I}_z(z \mathbf{i}_z + a \mathbf{i}_\rho, t) d\phi \quad (8)$$

that flows along the wire. The motivation for considering only the total current is that this quantity governs the behavior of the scattered field for  $\mathbf{r} \in \bar{\mathcal{D}}$  when  $|\mathbf{r} - \mathbf{r}'| \gg a$  for all  $\mathbf{r}' \in \partial\mathcal{D}$ . This is observed immediately by taking  $\mathbf{r}' = z' \mathbf{i}_z + \rho' \mathbf{i}_\rho$ , in (1)–(3) and carrying out a Taylor expansion in terms of  $\rho'/|\mathbf{r} - z' \mathbf{i}_z|$ .

### B. End Conditions

A common element of all simplifications to be discussed is the use of boundary conditions for  $\mathcal{I}(z, t)$  near the end faces at  $z = 0, L$ .

One way of obtaining these conditions is to consider the total radial current flowing through a circular contour  $\mathcal{E}_0$  of radius  $\rho_0$  as shown in Fig. 2. Using the definition (3) and the fact that  $\mathcal{I}(\mathbf{r}, t)$  is the limiting value upon approaching  $\partial\mathcal{D}$  from  $\bar{\mathcal{D}}$ , we can use Maxwell's equations

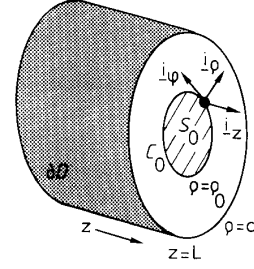


Fig. 2. Enlarged view of the end face of the wire at  $z = z_0 = L$  with circular contour  $\mathcal{E}_0$  and disk  $\mathcal{S}_0$  for definition and analysis of the radial current  $\mathcal{I}_\rho(z_0, \rho_0, t)$  defined in (9).

in  $\bar{\mathcal{D}}$  and Stokes' theorem to arrive at

$$\begin{aligned} \mathcal{I}_\rho(z_0, \rho_0, t) \stackrel{\text{def}}{=} - \oint_{\mathcal{E}_0} \mathcal{I}_\rho(z_0 \mathbf{i}_z + \rho_0 \mathbf{i}_\rho, t) ds \\ = \epsilon \partial_t \int_{\mathcal{S}_0} \mathcal{E}_z(z_0 \mathbf{i}_z + \rho, t) dS(\rho) \quad (9) \end{aligned}$$

where  $0 \leq \rho_0 \leq a$  and  $z_0 = 0, L$ , and where  $\mathcal{S}_0$  is the disk encircled by  $\mathcal{E}_0$ . Since  $\mathcal{E}(\mathbf{r}, t)$  remains finite for all  $\mathbf{r}$  and  $t$ , it follows from (9) that

$$\mathcal{I}_\rho(z_0, \rho_0, t) = \mathcal{O}(\rho_0^2), \quad \text{as } \rho_0 \downarrow 0. \quad (10)$$

In view of the small radius of the wire, therefore, it seems reasonable to estimate

$$\mathcal{I}_\rho(z_0, \rho_0, t) \approx 0 \quad (11)$$

for  $0 \leq \rho_0 \leq a$  and  $z_0 = 0, L$ . Moreover, it follows from conservation of charge that  $\mathcal{I}(0, t) = -\mathcal{I}_\rho(0, a, t)$  and  $\mathcal{I}(L, t) = \mathcal{I}_\rho(L, a, t)$ . Hence, consistency requires that we also impose the end conditions

$$\mathcal{I}(z_0, t) \approx 0 \quad (12)$$

for  $z_0 = 0, L$ . If necessary, both (11) and (12) may be used as boundary conditions in drawing up the one-dimensional integral equation.

### C. Approximating the Vector Potential

Perhaps the most straightforward way to arrive at such an equation is to replace the vector potential  $\mathcal{A}(\mathbf{r}, t)$  by

$$\mathcal{A}(\mathbf{r}, t) \approx \mathbf{i}_z \int_0^L \frac{\mathcal{I}(z', t - R/c)}{4\pi R} dz' \quad (13)$$

with  $R \stackrel{\text{def}}{=} \sqrt{(z - z')^2 + \rho^2}$ . This so-called *reduced-kernel approximation* holds for  $\mathbf{r} \in \bar{\mathcal{D}}$ , provided that  $R \gg a$  for all values  $0 < z' < L$ . Consequently, it is applicable almost everywhere in  $\bar{\mathcal{D}}$  for determining the electric-field strength  $\mathcal{E}(\mathbf{r}, t)$  from the known space-time behavior of  $\mathcal{I}(z, t)$ .

In addition, the expression for  $\mathcal{E}(\mathbf{r}, t)$  obtained by substituting (13) in (1) constitutes, along with the corresponding expression for  $\mathcal{A}(\mathbf{r}, t)$ , a valid solution to Maxwell's equations for all  $\mathbf{r} \in \bar{\mathcal{D}}$ . Therefore, the desired

one-dimensional equation can be obtained by continuing the approximation (13) up to the wire, and enforcing the known value of  $\mathcal{E}_z(\mathbf{r}, t)$  for  $\rho = a$ . This involves the following steps.

- Consider the integral relation (1) for  $\mathcal{E}_z(\mathbf{r}, t)$  with  $\mathbf{r} \in \partial\mathcal{D}$  and use the boundary condition  $\mathcal{E}_z(\mathbf{r}, t) = 0$ .
- Consider the integral relation (1) for  $\mathcal{E}_z(\mathbf{r}, t)$ , with  $\mathbf{r} \in \overline{\mathcal{D}}$ , and take  $\mathbf{r}$  just inside the gap region.
- Take the limit for  $\delta \downarrow 0$ , using (6).

Carrying out these steps produces the approximate integro-differential equation

$$-\epsilon \partial_t \mathcal{V}(t) \delta(z - z_g) - \epsilon \partial_t \mathcal{E}_z^i(z \mathbf{i}_z + a \mathbf{i}_\rho, t) = \left[ \partial_z^2 - \frac{1}{c^2} \partial_t^2 \right] \int_0^L \frac{\mathcal{A}(z', t - R_a/c)}{4\pi R_a} dz' \quad (14)$$

where  $R_a \stackrel{\text{def}}{=} \sqrt{(z - z')^2 + a^2}$ . This integral equation is internally inconsistent, since the value for the total current  $\mathcal{A}(z, t)$  depends on the direction of  $\mathbf{i}_\rho$ . To overcome this problem, we require that the electric-field component  $\mathcal{E}_z^i(z \mathbf{i}_z + a \mathbf{i}_\rho, t)$  be independent of  $\phi$  for  $0 \leq z \leq L$ . This is achieved by introducing the additional approximation

$$\mathcal{E}_z^i(z \mathbf{i}_z + a \mathbf{i}_\rho, t) \approx \mathcal{E}_z^i(z \mathbf{i}_z, t) \quad (15)$$

which is comparable in accuracy with concentrating the entire current on the central axis of the wire. This leads to the one-dimensional integro-differential equation

$$-\epsilon \partial_t \mathcal{V}(t) \delta(z - z_g) - \epsilon \partial_t \mathcal{E}_z^i(z \mathbf{i}_z, t) = \left[ \partial_z^2 - \frac{1}{c^2} \partial_t^2 \right] \int_0^L \frac{\mathcal{A}(z', t - R_a/c)}{4\pi R_a} dz' \quad (16)$$

which holds for  $0 \leq z \leq L$  and for  $t_0 \leq t < \infty$ .

At first glance, (16) appears to be an acceptable integral equation. Nevertheless, the objection remains that the underlying approximation (13) breaks down for  $z' - z = \mathcal{O}(a)$ , where the integrand assumes its largest magnitude. Because of this objection, (16) has been known in the literature as the *approximate form* or as the *reduced form* of Pocklington's integral equation.

#### D. Approximating the Current Density

Ostensibly, a more responsible approach for obtaining a one-dimensional integral equation is to consider the wire as an open-ended perfectly conducting tube, along which the current density is given by

$$\mathcal{J}(z \mathbf{i}_z + a \mathbf{i}_\rho, t) \approx \frac{\mathcal{A}(z, t)}{2\pi a} \mathbf{i}_z. \quad (17)$$

Substituting this approximation in (1) and going through the same steps that led to (16) results in

$$-\epsilon \partial_t \mathcal{V}(t) \delta(z - z_g) - \epsilon \partial_t \mathcal{E}_z^i(z \mathbf{i}_z, t) = \left[ \partial_z^2 - \frac{1}{c^2} \partial_t^2 \right] \int_0^L \int_0^\pi \frac{\mathcal{A}(z', t - R_\phi/c)}{4\pi^2 R_\phi} d\phi dz' \quad (18)$$

where  $R_\phi \stackrel{\text{def}}{=} \sqrt{(z - z')^2 + 4a^2 \sin^2 \phi}$  is the distance between two points on  $\partial\mathcal{D}$ . Like (16), this integral equation holds for  $0 < z < L$  and for  $t_0 \leq t < \infty$ .

Compared with the derivation of (16) given in Section II-C, the present one has the advantage that the *exact kernel* is used. In addition, the interpretation of the thin wire as an open-ended conducting surface leads to the conclusion that the end condition (12) is exact. Because of these features, (18) has been known in the literature as the *exact form* of Pocklington's equation. This equation has been the subject of careful theoretical [8], [9] and numerical [10]–[13], [23] studies by a number of investigators. As in the case of (16), the principal objection is that enforcing the underlying approximation (17) in the integrand of (1) for  $\mathbf{r} \in \partial\mathcal{D}$  and  $|\mathbf{r}' - \mathbf{r}| = \mathcal{O}(a)$  may have an undue influence of the value of the surface integral.

#### E. Exact Derivation

The classical derivations given in Sections II-C and II-D share the drawback that, in order to obtain a consistent integro-differential equation for  $\mathcal{A}(z, t)$ , the  $z$ -component of the incident electric field on the boundary of the wire must be approximated by the corresponding value on the central axis. This suggests that it may be more appropriate to consider the  $z$ -component of the integral relation (1) on that axis directly. For  $\delta \downarrow 0$ , this component is given by

$$-\epsilon \partial_t \mathcal{V}(t) \delta(z - z_g) - \epsilon \partial_t \mathcal{E}_z^i(z \mathbf{i}_z, t) = \left\{ \partial_z \nabla \cdot \mathcal{A}(\mathbf{r}, t) - \frac{1}{c^2} \partial_t^2 \mathcal{A}_z(\mathbf{r}, t) \right\} \Big|_{\mathbf{r}=z \mathbf{i}_z}, \quad (19)$$

with  $0 < z < L$ .

The essential difference between (19) and the integral equations (16) and (18) is the occurrence of transverse derivatives of  $\mathcal{A}(\mathbf{r}, t)$  with respect to  $\mathbf{r}$  in the first term on the right-hand side. These derivatives, however, can be shown to vanish. To this end, the gradient operator is broken up into  $\nabla = \nabla_T + \mathbf{i}_z \partial_z$ . By a straightforward differentiation of (2), it follows that

$$\nabla_T \cdot \mathcal{A}(\mathbf{r}, t) = \oint_{\partial\mathcal{D}} \left[ \frac{1}{R} + \frac{1}{c} \partial_t \right] (\boldsymbol{\rho}' - \boldsymbol{\rho}) \cdot \frac{\mathcal{A}(\mathbf{r}', t - R/c)}{4\pi R^2} dS(\mathbf{r}'). \quad (20)$$

Combining this expression with

- the fact that  $\boldsymbol{\rho} = \mathbf{0}$  on the wire axis,
- the estimate (11) for the total radial current on the end faces,
- The feature that  $\boldsymbol{\rho}' \cdot \mathcal{A}(\mathbf{r}', t) = 0$  on the remainder of  $\partial\mathcal{D}$ ,

leads to the conclusion that  $\{\nabla_T \cdot \mathcal{A}(\mathbf{r}, t)\}|_{\mathbf{r}=z \mathbf{i}_z} = 0$  for  $-\infty < z < \infty$ .

This leaves the  $z$ -component of the vector potential to be elaborated. We arrive at

$$\begin{aligned} \mathcal{A}_z(z\mathbf{i}_z, t) &\stackrel{\text{def}}{=} \oint_{\partial\mathcal{D}} \frac{\mathcal{F}_z(\mathbf{r}', t - R/c)}{4\pi R} dS(\mathbf{r}') \\ &= \int_0^L \frac{\mathcal{A}(z', t - R_a/c)}{4\pi R_a} dz' \end{aligned} \quad (21)$$

for  $-\infty < z < \infty$ . In (21), the total current  $\mathcal{A}(z, t)$  is defined according to (8), and  $R_a \stackrel{\text{def}}{=} \sqrt{(z - z')^2 + a^2}$ .

Substituting the two intermediate results obtained above in (19) produces the desired one-dimensional equation for  $\mathcal{A}(z, t)$ . Surprisingly, this equation turns out to be identical to the *approximate form* (16) of Pocklington's equation derived in Section II-C. This implies that, with the present discussion, we have given an almost exact derivation of that equation. The only approximation has been the introduction of (11). In Section II-B, that estimate was obtained directly from Maxwell's equations. Moreover, (11) is a local approximation that is noticed in (19) only when  $\mathbf{r}$  is located within a distance of  $\mathcal{O}(a)$  from the end faces. In that region, we have  $\mathcal{A}(z, t) = \mathcal{O}(a)$ . Consequently, imposing (11) has a negligible effect on the unknown current  $\mathcal{A}(z, t)$  in the interval  $0 < z < L$ . On the other hand, imposing (11) does have the consequence that, in the numerical computation, evaluating  $\mathcal{A}(z, t)$  in the immediate vicinity of the end faces ought to be avoided. Instead, the discretization of the integral over  $z'$  in (16) should be organized such that (11) is accounted for implicitly. This point will be addressed in more detail in Sections IV and V.

The integral equation (16) only describes the *total* current in the  $z$ -direction. No information is obtained about the angular distribution of  $\mathcal{F}_z$ , about the transverse current  $\mathcal{F}_\phi$ , or about the current distribution on the end faces. Furthermore, there are an infinite number of incident fields that give rise to the same total current  $\mathcal{A}(z, t)$ . As stated towards the end of Section II, this implies that all of these fields excite approximately the same scattered field away from the wire.

The idea of using a boundary integral representation with the point of observation inside a perfectly conducting scatterer is not new. In optics, the representation (1) with  $\mathbf{r} \in \mathcal{D}$  is known as Oseen's extinction theorem [31], [32]. This representation has been used as early as [33] to formulate an integral equation for the total current on an antenna with a cylindrical geometry and excitation. Later, it has been the basis of the so-called *null-field method* [34] and the *T-matrix methods* [35]. Nevertheless, the relevance of this idea for the formulation of the thin-wire problem has until now been overlooked.

Finally, the derivation outlined above warrants the conclusion that the so-called *approximate form* of Pocklington's equation is definitely superior to the so-called *exact form*. In the remainder of the manuscript, therefore, the discussion will be restricted to solving (16).

### III. THE ONE-DIMENSIONAL WAVE OPERATOR

Having established an "exact" space-time integral equation for  $\mathcal{A}(z, t)$ , we can now attempt to compute this current. Before we go into the numerical aspects, some attention must be devoted to the space and time differentiations occurring on the right-hand side of (16). In the literature, two different approaches have been proposed for handling these differentiations. In this section, we briefly discuss each of them.

#### A. Explicit Evaluation

One of the advantages of the integral equation (16) over its counterpart (18) is that, in the former, we have  $R_a \geq a$ . This means that, at least theoretically, there is no objection against evaluating the space and time derivatives explicitly.

To keep the discussion tractable, we first consider the evaluation of a single space derivative. Using the fact that  $\partial_z R_a = -\partial_z R_a$ , we find

$$\begin{aligned} \partial_z \mathcal{A}_z(z\mathbf{i}_z, t) &= - \int_0^L \partial_z \left\{ \frac{\mathcal{A}(z', t - R_a/c)}{4\pi R_a} \right\} dz' \\ &\quad - \int_0^L \frac{\partial_t q(z', t - R_a/c)}{4\pi R_a} dz'. \end{aligned} \quad (22)$$

In (22),  $q(z, t)$  denotes the total surface charge per unit length along the wire. In line with the definition (8), this quantity can be expressed as

$$\begin{aligned} q(z, t) &\stackrel{\text{def}}{=} -a \int_{t_0}^t \int_{-\pi}^{\pi} \partial_z \mathcal{F}_z(z\mathbf{i}_z + a\mathbf{i}_\rho, t') d\phi dt' \\ &= - \int_{t_0}^t \partial_z \mathcal{A}(z, t') dt'. \end{aligned} \quad (23)$$

In (22), the first term on the right-hand side is eliminated with the aid of the boundary conditions (12). Invoking these conditions does not introduce a new approximation since they are consistent with (11), which is the only approximation imposed in the "exact" derivation of (16). Removing this term is also allowed when  $\mathcal{A}(z, t)$  is discontinuous in  $z$ , provided that the  $z$ -derivative in (23) is interpreted in the sense of generalized functions.

The substitution of (22) in (16) results in an integral equation where all terms contain at least a single time differentiation. Using the initial conditions at  $t = t_0$ , we can integrate out this differentiation. This leaves a single space differentiation and a single time differentiation to be carried out. Performing these differentiations, we end up with

$$\begin{aligned} &\mathcal{V}(t) \delta(z - z_g) + \mathcal{E}_z^i(z\mathbf{i}_z, t) \\ &= \frac{1}{4\pi\epsilon} \int_0^L \left\{ \frac{1}{c^2 R_a} \partial_t \mathcal{A}(z', t - R_a/c) \right. \\ &\quad \left. - \frac{z - z'}{R_a^2} \left[ \frac{1}{R_a} + \frac{1}{c} \partial_t \right] q(z', t - R_a/c) \right\} dz'. \end{aligned} \quad (24)$$

The form (24) has been the basis of many applications of the *marching-on-in-time method* [16]–[19]. The most significant aspects of this method will be discussed in Section IV-A.

The main disadvantage of (24) lies in the numerical solution. In a typical discretization, the current distribution  $\mathcal{A}(z, t)$  is replaced by some local polynomial approximation in  $z$  and  $t$ . According to (24), this approximation is differentiated once with respect to space and/or time, and subsequently multiplied by an inverse power of  $R_a$ . The resulting approximate integrand is then integrated in closed form. Especially when  $z' \approx z$ , this procedure may amplify the individual interpolation errors. Further, the local approximations on adjoining subintervals should be connected such that the polynomial equivalent of  $\mathcal{A}(z, t)$  is continuous in  $z$ . Otherwise, enforcing the consistency relation (23) will give rise to unphysical delta-function contributions in the corresponding approximate version of the charge distribution  $q(z, t)$ .

### B. Hallén's Equation

Alternatively, the combination of space and time differentiations in (16) can be recognized as the differential operator governing the propagation of plane waves in a homogeneous, lossless dielectric. For that operator, the Green's function  $\mathcal{G}(z, t)$  can be defined as the causal solution of the inhomogeneous second-order differential equation

$$\left[ \partial_z^2 - \frac{1}{c^2} \partial_t^2 \right] \mathcal{G}(z, t) = -\delta(z) \delta(t). \quad (25)$$

This solution is given by

$$\mathcal{G}(z, t) = \frac{c}{2} \mathcal{W} \left( t - \frac{|z|}{c} \right) \quad (26)$$

where  $\mathcal{W}(t)$  is the unit time-step function [29]. Starting from (16) and (26) and using the superposition principle, we obtain by a straightforward convolution

$$\begin{aligned} & \int_0^L \frac{\mathcal{A}(z', t - R_a/c)}{4\pi R_a} dz' \\ &= \frac{Y}{2} \int_0^L \mathcal{E}_z^i \left( z' \mathbf{i}_z, t - \frac{|z - z'|}{c} \right) dz' \\ & \quad + \frac{Y}{2} \mathcal{W} \left( t - \frac{|z - z_g|}{c} \right) \\ & \quad + \mathcal{F}_0 \left( t - \frac{z}{c} \right) + \mathcal{F}_L \left( t - \frac{L - z}{c} \right) \end{aligned} \quad (27)$$

where  $0 < z < L$ , and where  $Y \stackrel{\text{def}}{=} \sqrt{\epsilon/\mu}$  denotes the wave admittance of the dielectric medium in  $\mathcal{D}$ . This equation is attributed to Hallén [2], [3], who employed it to develop an iterative solution procedure for determining  $\mathcal{A}(z, t)$ . For the special case of a straight thin-wire segment, an excellent account of this procedure was given by Bouwkamp [4]. The unknown time signals  $\mathcal{F}_0(t)$  and  $\mathcal{F}_L(t)$

represent two independent homogeneous solutions of the differential equation (25). These signals can be determined by invoking Hallén's equation for  $z = 0, L$  as well. This is allowed since the end conditions (12) must be imposed anyway, and since the integral on the left-hand side of (27) is a continuous function of  $z$ .

It has been argued [9] that Hallén's equation may be difficult to solve numerically. One explanation is that the unknown current  $\mathcal{A}(z, t)$  plays a different role than the unknown homogeneous solutions  $\mathcal{F}_0(t)$  and  $\mathcal{F}_L(t)$ . However, it is precisely because of this difference that the evaluation of the extra quantities  $\mathcal{F}_0(t)$  and  $\mathcal{F}_L(t)$  need not cause difficulties. In fact, their elimination from (27) is straightforward. Let

$$\begin{aligned} \mathcal{X}_0(t) &\stackrel{\text{def}}{=} \int_0^L \frac{\mathcal{A}(z, t - \sqrt{z^2 + a^2}/c)}{4\pi\sqrt{z^2 + a^2}} dz \\ & \quad - \frac{Y}{2} \int_0^L \mathcal{E}_z^i \left( z \mathbf{i}_z, t - \frac{z}{c} \right) dz - \frac{Y}{2} \mathcal{W} \left( t - \frac{z_g}{c} \right) \\ \mathcal{X}_L(t) &\stackrel{\text{def}}{=} \int_0^L \frac{\mathcal{A}(z, t - \sqrt{(L-z)^2 + a^2}/c)}{4\pi\sqrt{(L-z)^2 + a^2}} dz \\ & \quad - \frac{Y}{2} \int_0^L \mathcal{E}_z^i \left( z \mathbf{i}_z, t - \frac{L-z}{c} \right) dz \\ & \quad - \frac{Y}{2} \mathcal{W} \left( t - \frac{L-z_g}{c} \right). \end{aligned} \quad (28)$$

Then, the unknown time signals can be expressed as

$$\begin{aligned} \mathcal{F}_0(t) &= \sum_{n=0}^{\infty} \mathcal{X}_0 \left( t - \frac{2nL}{c} \right) - \sum_{n=0}^{\infty} \mathcal{X}_L \left( t - \frac{(2n+1)L}{c} \right) \\ \mathcal{F}_L(t) &= \sum_{n=0}^{\infty} \mathcal{X}_L \left( t - \frac{2nL}{c} \right) - \sum_{n=0}^{\infty} \mathcal{X}_0 \left( t - \frac{(2n+1)L}{c} \right). \end{aligned} \quad (29)$$

One way of proving this result is to take  $z = 0$  and  $z = L$  in (27), and to apply a temporal Laplace transformation. This leads to a system of two linear equations for the transforms of  $\mathcal{F}_0(t)$  and  $\mathcal{F}_L(t)$ . The substitution of (29) in (27), finally, gives a relatively complicated integral equation in which  $\mathcal{A}(z, t)$  is the only unknown. As mentioned above, the equation thus obtained must be solved in combination with the end conditions (12), and with initial conditions at  $t = t_0$ . From a computational point of view, this equation is completely equivalent to (27).

## IV. MARCHING ON IN TIME

Next, we turn our attention to the numerical solution of the integral equations (16), (24), or (27). The numerical evaluation of  $\mathcal{A}(z, t)$  can be performed in two ways. In the first place, the problem can be solved directly in the time domain, by using the common property in these integral equations that  $\mathcal{A}(z, t)$  at each space-time point is expressed in terms of one or more integrals of values  $\mathcal{A}(z', t')$  at previous instants. This requires a systematic

discretization in space and time. In the second place, we can use the property that the scattering problem in linear and time-invariant. Hence, a temporal Laplace transformation decomposes a space-time integral equation into a continuum of lower-dimensional equations in which the frequency occurs as a parameter. In the numerical solution of the transformed equations, only a space discretization is required. Both approaches lead to different implementations accordingly as Pocklington's or Hallén's equation is considered. In the present section, we discuss the direct time-domain solution. Frequency-domain techniques will be discussed in Section V.

#### A. Pocklington's Equation

The classical way to determine  $\mathcal{A}(z, t)$  directly in the time domain utilizes the elaborated form (24) of Pocklington's equation [15], [16], [19]. As mentioned in Section III-A, the unknown current in that equation is replaced by a polynomial approximation in  $z$  and  $t$ . This results in a discretized equation for approximate sampled values of  $\mathcal{A}(z, t)$  that can be solved recursively in (discretized) time. This procedure is known as the *marching-on-in-time method*. Since the numerical implementation has been well documented in [16], [19], we merely emphasize some significant details. The space-time discretization starts off with the introduction of a spatial grid. The interval  $0 < z < L$  is divided into  $M$  subintervals of equal length  $\Delta z \stackrel{\text{def}}{=} L/M$ , centered around the midpoints  $z_m \stackrel{\text{def}}{=} (m - 1/2)\Delta z$ , with  $m = 1, \dots, M$ . To incorporate the end conditions (12), this grid is extended with the points  $z_0 \stackrel{\text{def}}{=} 0$  and  $z_{M+1} \stackrel{\text{def}}{=} L$ . Next, the time coordinate is discretized according to  $t_n = t_0 + n\Delta t$ , with  $n = 0, 1, \dots, \infty$ . Generally, the time step  $\Delta t$  is chosen such that  $\Delta t \leq \Delta z/c$ .

In the region closest to the space-time point  $\{z_m, t_n\}$ , i.e., for space-time points with  $|z - z_m| < \Delta z/2$  and  $|t - t_n| < \Delta t/2$ , the current is approximated by a three-point Lagrangian interpolation polynomial in  $z$  and  $t$  of the form

$$\mathcal{I}_{m,n}(z, t) \approx \sum_{m'=m-1}^{m+1} \sum_{n'=n-l-1}^{n-l+1} \mathcal{A}(z_{m'}, t_{n'}) \mathcal{P}_{m,n}^{(m',n')}(z, t) \quad (30)$$

with

$$\mathcal{P}_{m,n}^{(m',n')}(z, t) \stackrel{\text{def}}{=} \prod_{\substack{m''=m-1 \\ m'' \neq m'}}^{m+1} \prod_{\substack{n''=n-l-1 \\ n'' \neq n'}}^{n-l+1} \frac{z - z_{m''}}{z_{m'} - z_{m''}} \frac{t - t_{n''}}{t_{n'} - t_{n''}} \quad (31)$$

where  $m = 1, \dots, M$  and  $n = 0, 1, \dots, \infty$ . In (30) and (31),  $l = 0$  when  $(n+1)\Delta t$  does not exceed the instant at hand, and  $l = 1$  otherwise. Thus, the quadratic time interpolation is central when possible and backward when necessary.

The approximation (30) is substituted into (24). Subsequently, the space and time differentiations and the space integration are performed analytically. In the space dif-

ferentiation, possible delta-function contributions at the boundaries of the spatial cells are neglected. Formally, such contributions should be taken into account, since the approximation in (30) and (31) is discontinuous at the boundaries of the subintervals. Enforcing the equality sign in the resulting discretized version of (24) at the collocation points  $z = z_m$  with  $m = 1, \dots, M$  and for  $t = t_n$  with  $n = 0, 1, \dots, \infty$  then results in a system of linear equations for the approximate sampled current values  $\mathcal{I}_m[n]$ . This system is lower-triangular in the time index  $n$ , and, hence, can be inverted recursively in  $n$ . The recurrence scheme is not explicit, but the system of linear equations that must be inverted to obtain the  $\{\mathcal{I}_m[n]\}$  for each instant  $n$  is sparse and independent of  $n$ . Therefore, we can either solve this system repeatedly using the sparsity, or compute the inverse of the system matrix once and store it, or combine both ideas by storing the LU-decomposition of the banded system matrix. In practice, the last possibility is often preferred.

The results obtained with the procedure described above agree well with data obtained by several alternative techniques [19]. Nevertheless, there are at least three problems with the space-time discretization. The first two are related to the space discretization. The problem of the delta-function terms in  $q(z, t)$  due to the discontinuities in the interpolation (30) and (31) has already been mentioned. In principle, it is not difficult to account for the contributions of these terms in (24). A more serious problem is the fact that the end conditions (12) are imposed at a distance of  $\Delta z/2$  from the nearest collocation point. As argued in Section II-E, (16) and equivalent forms should be invoked away from the end faces. In that context, it seems strange to refine the space discretization exactly at those end faces. Further, any irregularity in the space discretization may in itself give rise to numerical errors.

Either of these problems can explain the phenomenon that even minor changes in the discretization immediately cause instabilities in the time-domain results obtained. This phenomenon is not important in the problem at hand, but it does affect the treatment of wire junctions. It turns out that only a single junction condition leads to stable results [19].

The third problem originates from the time discretization. At each instant  $t = t_n$ , the integral equation (24) relates values of  $\mathcal{A}(z', t')$  with  $0 < z' < L$  and  $t' \leq t_n - a/c$  to known values of the incident field and the impressed voltage. In the marching-on-in-time method, the discretized counterpart is used to determine approximations to  $\mathcal{A}(z_m, t_n)$ . When  $\Delta t \leq a/c$ , this procedure becomes unstable because the weighting factors of the unknown current values at  $t = t_n$  are too small. The effect has, for example, been reported in [18]. To overcome this problem, (24) must be collocated at  $t = t_n + a/c$ .

#### B. Hallén's Equation

The direct time-domain solution of Hallén's equation has received less attention in the literature than the

solution of Pocklington's equation described above. The only implementation known to the authors is the one described in [36]. In that reference, the time delay  $R_a/c$  in the current integral on the left-hand side of (27) is approximated by  $|z - z'|/c$ , with a local correction in the "self-patch," i.e., in the cell containing the point of observation. A numerical solution of the "exact" equation (27) has not been reported.

We performed the space-time discretization according to the ideas developed in [30] and [37]. As in Section IV-A, the interval  $0 < z < L$  is subdivided into  $M$  subintervals of equal length  $\Delta z \stackrel{\text{def}}{=} L/M$ . The grid points are taken at the boundaries of the subintervals, i.e.,  $z_m = m\Delta z$ , with  $m = 0, \dots, M$ . In (27), the observation is restricted to the grid points  $z = z_m$ , with  $m = 0, \dots, M$ . The integral over the unknown current  $\mathcal{A}(z', t - R_a/c)$  is approximated by a weighted sum over the sampled values at  $z' = z_{m'}$ , with  $m' = 1, \dots, M - 1$ . To this end, we introduce the piecewise-linear approximation

$$\begin{aligned} \mathcal{A}(z', t - \sqrt{(m\Delta z - z')^2 + a^2}/c) \\ \approx \sum_{m'=1}^{M-1} \mathcal{A}(z_{m'}, t - R_{m-m'}/c) \phi_{m'}(z') \end{aligned} \quad (32)$$

where  $R_m \stackrel{\text{def}}{=} \sqrt{m^2\Delta z^2 + a^2}$ , and where  $\phi_m(z)$  is the triangular expansion function

$$\phi_m(z) \stackrel{\text{def}}{=} \begin{cases} 1 - |z - z_m|/\Delta z, & \text{for } |z - z_m| \leq \Delta z \\ 0, & \text{otherwise.} \end{cases} \quad (33)$$

This approximation interpolates on a regular grid, and implicitly accounts for the end conditions (12). This means that the first two problems mentioned in Section IV-A have been circumvented. The equations with  $m = 0$ ,  $M$  have been included for the computation of the auxiliary signals  $\mathcal{F}_0(t)$  and  $\mathcal{F}_L(t)$ .

For plane-wave incidence, the integral over  $\mathcal{E}_z^i(z', \mathbf{i}_z, t - |z - z'|/c)$  on the right-hand side of (27) is calculated in closed form. For more general incident fields, this integral is evaluated with the aid of a repeated trapezoidal rule over the abscissae  $\{z_m\}$ . This quadrature rule is of a similar accuracy as the piecewise linear approximation (32).

With these approximations, the space-time integral equation (27) reduces to the system of linear time-domain equations

$$\begin{aligned} \sum_{m'=1}^{M-1} W_{m-m'} I_{m'}(t - R_{m-m'}/c) \\ = \frac{Y}{2} \sum_{m'=0}^M w_{m'} \mathcal{E}_z^i \left( z_{m'} \mathbf{i}_z, t - \frac{|z_m - z_{m'}|}{c} \right) \\ + \frac{Y}{2} \mathcal{Z} \left( t - \frac{|z_m - z_g|}{c} \right) \\ + \mathcal{F}_0 \left( t - \frac{z_m}{c} \right) + \mathcal{F}_L \left( t - \frac{L - z_m}{c} \right) \end{aligned} \quad (34)$$

from  $m = 0, \dots, M$ . In the generalized trapezoidal rule on the left-hand side, the weighting coefficients are defined as

$$W_m \stackrel{\text{def}}{=} \int_{z_m - \Delta z}^{z_m + \Delta z} \frac{\phi_m(z)}{\sqrt{z^2 + a^2}} dz \quad (35)$$

for  $m = 0, \pm 1, \dots, \pm(M - 1)$ . These coefficients are available in closed form. In the trapezoidal rule on the right-hand side, we have  $w_m \stackrel{\text{def}}{=} \Delta z$  for  $m = 1, \dots, M - 1$ , and  $w_0 = w_M \stackrel{\text{def}}{=} \Delta z/2$ . Equation (34) with  $t \geq t_0$  constitutes a system of linear time-domain equations of dimension  $M - 1$  for the unknown time signals  $\{\mathcal{F}_m(t)\}$ , which are defined as the exact solutions of the space-discretized equation. These time signals, in turn, are the counterparts of the sampled field values  $\{\mathcal{A}(z_m, t)\}$ .

Next, the time coordinate is discretized according to  $t = t_0 + n\Delta t$ , with  $n = 0, 1, \dots, \infty$ . In the system of equations (34), the observation is limited to the instants  $t = t_n + a/c$ . To handle the time delays in the auxiliary signals  $\mathcal{F}_0(t)$  and  $\mathcal{F}_L(t)$ , these signals are interpolated linearly in between these instants. The unknown time signals  $\{\mathcal{F}_m(t)\}$  are approximated by piecewise-linear interpolation between the instants  $t = t_n$ . In this manner, the third problem mentioned in Section IV-A is avoided as well. In the terms containing the known incident field and the impressed voltage, no interpolation is necessary. As in the case of Pocklington's equation, the time discretization results in a system of linear equations for the unknown sampled current values  $\mathcal{F}_m[n] \approx \mathcal{A}(z_m, t_n)$  and the unknown sampled auxiliary signals  $\mathcal{F}_0[n] \approx \mathcal{F}_0(t_n + a/c)$  and  $\mathcal{F}_L[n] \approx \mathcal{F}_L(t_n + a/c)$ . This system is solved recursively in  $n$ .

Finally, some attention should be devoted to the choice of the time step  $\Delta t$ . For  $\Delta t \leq \Delta z/c$ , the evaluation of  $\mathcal{F}_0[n]$  and  $\mathcal{F}_L[n]$  is explicit, and thus independent of the values of  $\{\mathcal{F}_m[n]\}$  at the same  $n$ . The evaluation of  $\mathcal{F}_m[n]$  is explicit only when  $c\Delta t \leq \sqrt{\Delta z^2 + a^2} - a$ . For mesh sizes of length  $\Delta z = \mathcal{O}(a)$  or larger, this condition is easily satisfied. As  $\Delta z \downarrow 0$ , however, time steps of length  $c\Delta t = \mathcal{O}(\Delta z^2/a)$  are needed. As a consequence, the marching-on-in-time computation becomes increasingly time-consuming. In that case, it is more efficient to invert a banded Toeplitz matrix of dimension  $M - 1$  to find the unknown values of  $\mathcal{F}_m[n]$  for each  $n$ . Numerical experimentation has shown that this does not cause instabilities, as long as  $M$  is not chosen unnecessarily large.

## V. FREQUENCY-DOMAIN TECHNIQUES

A possible disadvantage of the marching-on-in-time method is that, even when stable results are obtained, the errors introduced by the discretization accumulate as the computation progresses. As a consequence, these errors are typically amplified by a "statistical" factor of  $\mathcal{O}(\Delta t^{-1/2})$ . This disadvantage is avoided when the problem is considered in the time-Laplace domain.



This amounts to carrying out the temporal Laplace transformation

$$I(z, s) \stackrel{\text{def}}{=} \int_{t_0}^{\infty} \mathcal{A}(z, t) \exp(-st) dt \quad (36)$$

where  $s$  denotes a complex angular frequency with  $\text{Re}(s) \geq 0$ . The corresponding inverse transformation is given by

$$\mathcal{A}(z, t) = \frac{1}{2\pi} \exp(\beta t) \int_{-\infty}^{\infty} I(z, \beta + i\omega) \exp(i\omega t) d\omega \quad (37)$$

with  $\beta \geq 0$ . Numerically,  $\mathcal{A}(z, t)$  can be evaluated from the known values of  $I(z, \beta + i\omega)$  with the aid of the so-called fast Fourier transformation (FFT).

The Laplace transformation reduces the solution of a given space-time integral equation to the repeated solution of a lower-dimensional equation and the evaluation of the inversion integral in (37). Traditionally, the transform  $I(z, \beta + i\omega)$  is determined with a constant relative accuracy for all frequencies  $-\infty < \omega < \infty$ . This requires a space discretization with a mesh size  $\Delta z = \mathcal{O}(\omega^{-1})$  as  $|\omega| \rightarrow \infty$ . The major drawback of doing this is that the computational effort required to determine a single constituent becomes proportional to some positive power of  $|\omega|$ .

Recently [30], it was observed that accurate time-domain results can be obtained as well by choosing a *fixed* space discretization with a mesh size  $\Delta z$  much longer than the one used in "conventional" computations. This surprising result can be understood in two ways. From a frequency-domain point of view, the explanation is that  $I(z, \beta + i\omega)$  contains the spectrum of the incident pulse and/or the impressed voltage. Apparently, the decrease of the spectral amplitude(s) as  $\omega \rightarrow \infty$  compensates the increase of the relative error. Acceptable time-domain results are obtained as long as the *total* error in  $I(z, \beta + i\omega)$  leads to an integrable contribution in (37). Moreover, the error in the time-domain results is still of  $\mathcal{O}(\Delta z^m)$ , with  $m$  a positive integer. From a time-domain point of view, the explanation is derived from the success of the marching-on-in-time method. As described in Section IV, that method introduces a fixed space discretization at each instant, and, subsequently, a time discretization. The approach outlined above can be regarded as solving the space-discretized integral equation in continuous time. This has led to the designation *continuous-time discretized-space* (CTDS) *approach*. For illustrative examples and a more detailed explanation, the reader is referred to [30].

In the present section, we consider both points of view. First, Pocklington's equation (16) is transformed to the time-Laplace domain and discretized by a simple frequency-domain procedure. Next, the discretized counterpart (34) of Hallén's equation is transformed and solved iteratively with a special version of the conjugate-gradient method.

### A. Pocklington's Equation

In most frequency-domain computations, the fundamental integral equation is the transformed counterpart of (16), i.e.,

$$-s\epsilon V(s)\delta(z - z_g) - s\epsilon E_z^i(z\hat{\mathbf{i}}_z, s) = \left[ \partial_z^2 - \frac{s^2}{c^2} \right] \int_0^L \frac{\exp(-sR_a/c)}{4\pi R_a} I(z', s) dz'. \quad (38)$$

To demonstrate the potentialities of the CTDS approach, we have discretized this equation by the simplest form of the "standard" procedure due to Wilton and Butler [13]. These authors multiply (38) by a triangular expansion function as defined in (33), and use the result

$$\begin{aligned} & \int_{-\infty}^{\infty} \phi_m(z) \partial_z^2 \psi(z) dz \\ &= \int_{-\infty}^{\infty} \psi(z) \partial_z^2 \phi_m(z) dz \\ &= \frac{\psi(z_{m+1}) - 2\psi(z_m) + \psi(z_{m-1}))}{\Delta z} \end{aligned} \quad (39)$$

where  $z_m = m\Delta z$  with  $m = 0, \dots, M$ , and where  $\psi(z)$  is a two times differentiable function of  $z$ . Thus, the second-order differentiation with respect to  $z$  in the right-hand side of (38) is reduced in closed form to a difference rule. The integrals over the scalar terms in (38) are approximated by

$$\int_{-\infty}^{\infty} \phi_m(z) \psi(z) dz = \Delta z \psi(z_m) + \mathcal{O}(\Delta z^2) \quad (40)$$

as  $\Delta z \downarrow 0$ . The delta-function term in (38) gives rise to a weighted sum of two triangular expansion functions, sampled at  $z = z_g$ . With this result and (30) and (40), the discretization is reduced to evaluating the integral over  $I(z', s)$  on the right-hand side of (38).

Owing to the elegant reduction of the space differentiation, this integral may be discretized by taking the unknown current distribution piecewise constant in subintervals centered around the sample points. We assume that  $I(z', s) \approx I_{m'}(s)$  for  $|z' - z_{m'}| < \Delta z/2$  with  $m' = 0, \dots, M$ . As prescribed by the end conditions (12), we take  $I_0(s) = I_M(s) = 0$ . We then obtain

$$\begin{aligned} & \int_0^L \frac{\exp(-sR_a/c)}{4\pi R_a} I(z', s) dz' \\ & \approx \sum_{m'=1}^{M-1} I_{m'}(s) \int_{z_{m'} - \Delta z}^{z_{m'} + \Delta z} \frac{\exp(-sR_a/c)}{4\pi R_a} dz'. \end{aligned} \quad (41)$$

The integrals over the subintervals around  $z = z_{m'}$  with  $m' = 0, \dots, M$  are computed for  $z = z_m$  with  $m = 1, \dots, M - 1$  by changing the integration variable to  $z' - z_m$ . This results in  $M + 1$  different integrals that are evaluated

- by replacing the factor of  $\exp(-sR_a/c)$  with the three-term Taylor approximation  $1 - sR_a/c + (1/2)$

$(sR_a/c)^2$  in the self-cell, and integrating the result analytically;

- by numerical integration over the nearest and next-nearest neighbor cells;
- by the midpoint rule in the remaining subintervals.

Substituting the results derived above in (38) leads to a Toeplitz system of linear equations for the sampled current values  $\{I_m(s)\}$ . From this system, the  $\{I_m(s)\}$  can be determined efficiently with the aid of Levinson's algorithm [38, section 5.7].

Approximating  $I(z', s)$  by a piecewise constant function is less accurate than the piecewise-linear and piecewise-quadratic interpolations applied elsewhere in this paper. As a consequence, a larger number of subintervals is required. For the present discretization, this number typically lies between  $M = 100$  and  $M = 200$  for pulse widths in the range  $L/10 < c\tau < L$ . For higher order expansion functions, values between  $M = 30$  and  $M = 60$  suffice. This is the price we have to pay for obtaining the Toeplitz form of the system of linear equations for the  $\{I_m(s)\}$  and, hence, for being able to solve this system efficiently.

The procedure outlined above is carried out repeatedly for the complex frequencies  $s_n \stackrel{\text{def}}{=} \beta + in\Delta\omega$ ,  $n = 0, 1, \dots, N-1$ . The corresponding sampled time signals  $\mathcal{I}_m[n]$  are then obtained by evaluating the Bromwich inversion integral with the aid of an FFT algorithm. The parameters  $\beta$ ,  $\Delta\omega$ , and  $N$  are chosen such that the error introduced in this evaluation is negligible compared with the error caused by the space discretization. A possible strategy for choosing these parameters runs as follows:

1) Specify the time interval of interest  $t_0 < t < t_{\max}$ . To this end, some physical insight into the problem at hand is needed.

2) Since the inversion must be carried out with the aid of an FFT operation, this choice fixes the frequency step  $\Delta\omega = 2\pi/(t_{\max} - t_0)$ .

3) The number of samples  $N$  follows from the frequency content of the forcing function (incident field or impressed voltage). The time step  $\Delta t = (t_{\max} - t_0)/N$  is in practice chosen at least five times smaller than prescribed by Shannon's sampling theorem. The magnitude of the Laplace transform of the forcing function is then monitored to determine whether the remaining frequency constituents may be set to zero. In this manner, the FFT operation performs a Shannon-type interpolation at the cost of a minimal increase in computational effort.

4) The parameter  $\beta$  is chosen such that the factor of  $\exp(\beta t)$  in (37), by which the FFT results are multiplied, does not become excessively large over the time interval of interest. In practice,  $\exp[\beta(t_{\max} - t_0)] \approx 10$  is a suitable choice. If the presence of "interior modes" makes it necessary, this value can be increased up to  $\exp[\beta(t_{\max} - t_0)] \approx 100$ .

### B. Hallén's Equation

In [30], it was argued that a more direct implementation of the CTDS approach is obtained by carrying out the

space discretization as in the marching-on-in-time method, and transforming the result to the frequency domain. This has the additional advantage that the discretization error can be analyzed in the time domain. In our frequency-domain solution of Hallén's equation, we have followed this idea. The space-discretized equation (34) transforms into the system of linear equations

$$\begin{aligned} & \sum_{m'=1}^{M-1} W_{m-m'} \exp\left(-s \frac{R_{m-m'}}{c}\right) I_{m'}(s) \\ &= \frac{Y}{2} \exp\left(-s \frac{|z_m - z_g|}{c}\right) V(s) \\ &+ \frac{Y}{2} \sum_{m'=0}^M w_{m'} \exp\left(-s \frac{|z_m - z_{m'}|}{c}\right) E_z^i(z_{m'}, \mathbf{i}_z, s) \\ &+ \exp\left(-s \frac{z_m}{c}\right) F_0(s) + \exp\left(-s \frac{L - z_m}{c}\right) F_L(s) \end{aligned} \quad (42)$$

for  $m = 0, \dots, M$ . To arrive at this system, only a single approximation was needed, namely the piecewise-linear approximation (32). This makes it relatively easy to assess the discretization error. On the other hand, the occurrence of the terms involving  $F_0(s)$  and  $F_L(s)$  disturbs the Toeplitz structure of the system matrix. Therefore, Levinson's algorithm can no longer be applied.

We have solved the matrix equation (42) by a dedicated version of the conjugate-gradient method. The conjugate-gradient method as such is well documented and need not be discussed here. It has, for instance, been formulated in matrix form in [38, section 10.2] and in operator form in [39]. A careful analysis of several aspects of this method can be found in [40]. The new elements in our implementation are the evaluation of the direct and adjoint operators and the generation of the initial estimate.

To condense the notation, we rewrite (42) in matrix form as

$$\mathbf{A}(s) \cdot \mathbf{x}(s) = \mathbf{b}(s) \quad (43)$$

where  $\mathbf{A}(s)$  denotes a known  $(M+1) \times (M+1)$  matrix, and where  $\mathbf{x}(s)$  and  $\mathbf{b}(s)$  denote an unknown and a known vector of length  $M+1$ , respectively. The components of the unknown vector  $\mathbf{x}(s)$  are defined as

$$x_m(s) \stackrel{\text{def}}{=} \begin{cases} F_0(s), & \text{for } m = 0 \\ I_m(s), & \text{for } m = 1, \dots, M-1 \\ F_L(s), & \text{for } m = M. \end{cases} \quad (44)$$

With this definition, the matrix elements  $A_{m,m'}(s)$  and the known vector components  $b_m(s)$  are immediately read from (42). Further, we introduce the inner product of two vectors  $\mathbf{x}$  and  $\mathbf{y}$  as

$$\langle \mathbf{x} | \mathbf{y} \rangle \stackrel{\text{def}}{=} \sum_{m=0}^M \bar{x}_m y_m \quad (45)$$

where the overbar indicates complex conjugation. In terms of this inner product, the solution of (43) is redefined as

the vector that minimizes the squared error

$$\langle \mathbf{A}(s) \cdot \mathbf{x}(s) - \mathbf{b}(s) | \mathbf{A}(s) \cdot \mathbf{x}(s) - \mathbf{b}(s) \rangle. \quad (46)$$

We search this minimum by the standard conjugate-gradient procedure outlined in [38], [39]. In this procedure, the bulk of the computational effort is used up in the successive multiplications of the iterates with  $\mathbf{A}(s)$  and of the corresponding residuals with its adjoint. The efficiency of these multiplications improves considerably when the sum over  $m'$  on the left-hand side of (42) is recognized as a convolution that can be evaluated simultaneously for all relevant  $m$  with the aid of an FFT algorithm.

This possibility has been known since [25]–[27]. The new element in our version is that, in the context of the CTDS approach, we no longer regard (42) as a discretized integral equation. Instead, we simply treat it as a matrix equation that must be solved as accurately as possible. Hence, we organize the discrete convolution such that the left-hand side of (42) and its counterpart in the adjoint operator are evaluated *exactly*. This is achieved by using an FFT with an order of at least  $2M$ .

The most interesting aspect of our implementation is the generation of the initial guess. From (42)–(44), it is observed that, for a fixed order  $M + 1$ , both the matrix  $\mathbf{A}(s)$  and the known vector  $\mathbf{b}(s)$  are analytic functions of the frequency parameter  $s = \beta + i\omega$ . This means that, when  $\mathbf{A}(s)$  has a bounded inverse, the unknown vector  $\mathbf{x}(s)$  is analytic in  $s$  as well. Furthermore, performing the Bromwich inversion (37) as explained at the end of Section V-A requires the solution of the matrix equation for  $s_n = \beta + in\Delta\omega$ , with  $n = 0, \dots, N - 1$ , for a relatively short frequency step  $\Delta\omega$ . This suggests that we *march on in frequency*, using the analytic behavior of  $\mathbf{x}(s)$  to generate the successive initial estimates  $\mathbf{x}^{(0)}(s_n)$  from which the conjugate-gradient procedure is started.

After extensive experimentation, the following extrapolation scheme was found to be the most effective. For each new frequency  $s_n$ , the initial guess is expressed as a linear combination of previous “final” results

$$\mathbf{x}^{(0)}(s_n) \stackrel{\text{def}}{=} \sum_{k=1}^K \alpha_k \mathbf{x}(s_{n-k}). \quad (47)$$

The expansion coefficients  $\{\alpha_k\}$  are chosen such that the initial guess minimizes the squared error (46). This means that these coefficients follow from the system of linear equations

$$\begin{aligned} \sum_{k'=1}^K \langle \mathbf{A}(s_n) \cdot \mathbf{x}(s_{n-k'}) | \mathbf{A}(s_n) \cdot \mathbf{x}(s_{n-k}) \rangle \alpha_{k'} \\ = \langle \mathbf{A}(s_n) \cdot \mathbf{x}(s_{n-k}) | \mathbf{b}(s_n) \rangle \end{aligned} \quad (48)$$

where  $k = 1, \dots, K$ . The best results were obtained for  $K = 3$ , which corresponds to “quadratic” extrapolation. For a typical choice of  $\Delta\omega$ , the computation of a single frequency-domain constituent  $\mathbf{x}(s_n)$  then took about 1–5 iteration steps of the conjugate-gradient FFT method,

with peaks of 10–15 steps near the resonant frequencies. By taking a smaller  $\Delta\omega$ , it is possible to reduce the number of iterations per constituent still further. However, in view of the evaluation of the  $\{\mathbf{A}(s_n) \cdot \mathbf{x}(s_{n-k})\}$  for  $k = 1, \dots, K$ , carrying out 1–5 steps per frequency leads to a faster overall computation. Starting from a zero initial guess took about  $M/3$  iterations per constituent. For a more detailed discussion of the marching-on-in-frequency approach, the reader is referred to [41].

While our research was in progress, a similar idea was published in [42] for the case of monochromatic plane-wave illumination at multiple angles of incidence. In [42], previous conjugate-gradient directions are used in an expansion as summarized in (47) and (48). In the matrix formulation of (43), the multiple-incidence problem amounts to changing only the known vector  $\mathbf{b}(s)$ , and computing the corresponding solution  $\mathbf{x}(s)$ . The multiple-frequency problem is essentially more difficult, since the matrix  $\mathbf{A}(s)$  changes as well. This makes it even more surprising that a good initial guess can be generated with a few expansion functions that are independent of  $\mathbf{A}(s_n)$ . The largest surprise, however, is that the conjugate-gradient method is sensitive to the initial guess. This contradicts the existing experience of many authors (for the thin-wire case, see, e.g., [43]). This conclusion is corroborated by the observation that the number of iterations is influenced by the choice of  $\Delta\omega$ .

## VI. NUMERICAL RESULTS

As stated in the introduction, numerical results obtained with some of the algorithms described in this paper have already been published elsewhere. In particular, results of solving Pocklington’s equation by marching on in time are given in [19] and results of solving Hallén’s equation by marching on in frequency can be found in [41].

In the present context, it seems appropriate to compare the four algorithms. We have performed a number of numerical experiments for varying wire dimensions  $L$  and  $a$ , and for pulse durations in the range specified in Section V-A, i.e.,  $L/10 < c\tau < L$ . The following general observations can be made:

- Each of the algorithms approaches a fixed result when the number of space intervals  $M$  is increased. However, the “limiting values” are not identical. Typically, the result obtained by DOTIG1 (Pocklington, time marching) exhibits a slightly faster time variation than the result of solving Hallén’s equation by marching on in time. The results of both frequency-domain methods remain in between these signals. The differences decrease when the wire radius  $a$  is reduced. A possible explanation of this phenomenon is that a different local approximation of  $\mathcal{A}(z, t)$  introduces a different “effective length” of the wire segment. This phenomenon cannot be attributed to the use of the end conditions (12) in solving Hallén’s equation, since deviations are observed as well between different solutions of the same integral equation.

- The four solution procedures were implemented by three different authors, and the implementations were not equally optimized. Nevertheless, the conclusion seems justified that solving Hallén's equation directly in the time domain is considerably more efficient than the other procedures. Surprisingly, solving Pocklington's equation via the frequency domain comes second in efficiency, in spite of the larger value of  $M$  required because of the relatively crude space discretization. We attribute this to the relative efficiency of Levinson's algorithm for solving a system of linear equations, compared with the CGFFT procedure and the LU-decomposition employed in the other implementations. Obviously, this conclusion may change when different values of  $M$  are considered.

- For three of the methods outlined in this paper, numerical problems were experienced when the number of space intervals  $M$  was chosen excessively large. Apparently, choosing  $M$  too large allows some of the higher order resonances of the wire to show up as instabilities. Only for the frequency-domain solution of Pocklington's equation described in Section V-A, this effect was not observed.

As an illustration, the four methods discussed in this paper are compared for the case of an electrically polarized, pulsed plane wave normally incident on a wire with dimensions  $L = 1$  m and  $a = 2$  mm. The pulse shape is Gaussian, with approximate duration  $\tau = 0.3$  ns. A plane-wave excitation was selected to avoid the interpretation of the delta-function source in (16), which complicates the solution of Pocklington's equation for the case of gap-driven excitation. In addition, a relatively short pulse was chosen to demonstrate the length effect mentioned above.

Computational data of applying the four different methods have been summarized in Table I. For the frequency-domain applications, an FFT of order 2048 was carried out for a time step of  $\Delta t = 5/90$  ns. The real part of  $s_n = \beta + in\Delta\omega$  was  $\beta = 0$  for Pocklington's equation and  $\beta L/c = 0.1$  for Hallén's equation. The computation times refer to a VAX 3100/76 workstation with a relative performance of 7.6 VUP's.

The time signals obtained are given in Fig. 3. In this figure, the difference in time variation is clearly visible. To illustrate this difference in more detail, the maximum deviation between the four signals is shown in Fig. 4. Comparing Figs. 3 and 4 gives an additional justification of our interpretation of these deviations in terms of a different effective length. At early times, the largest deviation is observed when the current changes sign due to reflections at the ends of the wire segment. At late times, the accumulated effect of repeated reflections causes a time-spreading of the deviation.

Finally, the convergence of the marching-on-in-frequency approach described in Section V-B is illustrated in Fig. 5. In this figure, the number of iterations required for the CGFFT procedure to reach an RMS error of  $10^{-3}$  is shown for frequencies up to  $f = \omega/2\pi = 1$  GHz. In the computation leading to Fig. 3, the solution of (42) was

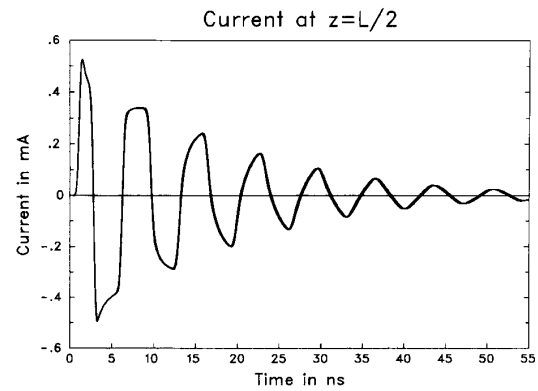


Fig. 3. Total current  $\mathcal{A}(L/2, t)$  on a wire with dimensions  $L = 1$  m and  $a = 2$  mm, excited by a normally incident, electrically polarized Gaussian pulse of approximate duration  $\tau = 0.3$  ns, obtained with four different solution procedures.

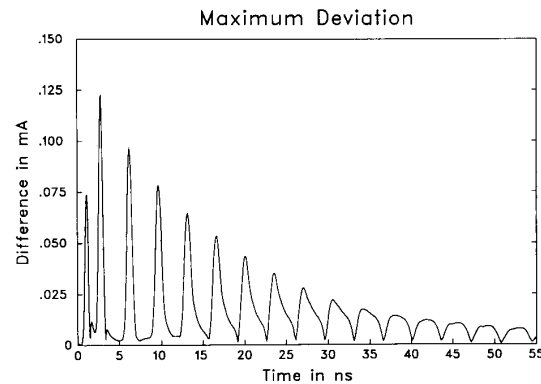


Fig. 4. Maximum deviation between the four time signals shown in Fig. 3 as a function of time.

TABLE I  
COMPUTATIONAL DATA OF EMPLOYING THE FOUR SOLUTION PROCEDURES DESCRIBED IN THIS PAPER TO THE TRANSIENT SCATTERING OF AN ELECTRICALLY POLARIZED, PULSED PLANE WAVE OF APPROXIMATE DURATION  $\tau = 0.3$  NS BY A WIRE SEGMENT OF LENGTH  $L = 1$  M AND RADIUS  $a = 2$  MM

Equation	Domain	$M$	CPU Time
Pocklington	Time	40	7 min 16 s
Hallén	Time	40	12 s
Pocklington	Frequency	100	1 min 22 s
Hallén	Frequency	60	2 min 02 s

continued up to  $f = 3.2$  GHz, with similar results. From Fig. 5, it is observed that the solution procedure loses efficiency near the resonant frequencies corresponding to "even" natural-mode current distributions, i.e., for  $f \approx (2n + 1) \times 150$  MHz with  $n = 0, 1, \dots, \infty$ . The convergence problems originate from the feature that the condition of the system matrix of a discretized integral equation deteriorates in the vicinity of a natural frequency. The

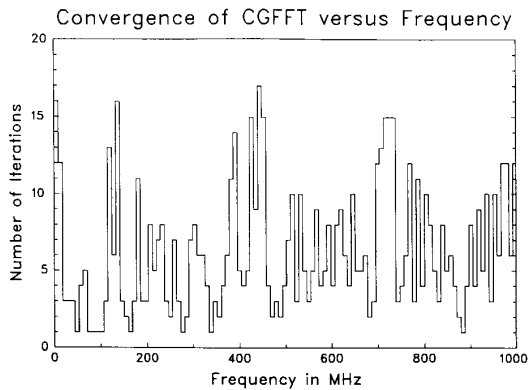


Fig. 5. Number of iterations required to reach an RMS error of  $10^{-3}$  versus frequency for the marching-on-in-frequency version of the CGFFT method. The results were obtained for the configuration specified in Fig. 3, for  $M = 60$  and  $\beta L/c = 0.1$ .

special role of the “even” modes corresponds to the choice of a symmetric excitation.

To appreciate the result shown in Fig. 5, the reader should be aware that a similar procedure starting from a zero initial estimate takes approximately  $M/3 = 20$  steps for each frequency. As explained in Section V-B, the number of iterations can be reduced still further by choosing a smaller frequency step  $\Delta\omega$ . However, the generation of more initial estimates for the CGFFT computations then leads to a longer overall computation time.

## VII. CONCLUSIONS

In this paper, we have given a new almost exact derivation of the integral equation governing the excitation of a straight thin-wire segment with a circular cross section. The only approximation is that the total current in the radial direction on the end faces is neglected. This approximation has been justified independently from Maxwell’s equations. Our derivation shows that Pocklington’s equation for the approximate or reduced kernel is almost exact, while the version for the exact kernel is approximate.

Next, we have analyzed a number of numerical solution techniques in the light of our new derivation. We distinguish between time-domain techniques and frequency-domain techniques. For each category, we have considered a “standard” implementation for solving Pocklington’s equation and a new implementation for solving Hallén’s equivalent form. The time-domain discretization of Pocklington’s equation developed in [16] and [19] has the disadvantage that the local polynomial approximation for the unknown current violates the continuity condition used in carrying out the space differentiations. Further, the space-time collocation takes place too close to the end faces and at the wrong instants. For Hallén’s equation, successive linear space and time interpolations were organized such that these problems are avoided.

In our frequency-domain implementation, we have followed the idea proposed in [30] of using a fixed space

discretization for all relevant frequencies. For Pocklington’s equation, we employed a simple form of the “standard” discretization of [13], and we used Levinson’s algorithm to solve the resulting Toeplitz system of linear equations. For Hallén’s equation, we transformed the space-discretized time-domain integral equation to the frequency domain. The system of equations obtained in this manner was solved by a dedicated version of the conjugate-gradient method. This has led to the second new result of the present research, i.e., the generation of successive initial estimates by marching on in frequency.

The comparison between both forms of the integral equation is somewhat biased by the fact the numerical schemes for solving Hallén’s equation were developed after our new derivation had become available. Nevertheless, it seems fair to conclude that our results agree with the common opinion that numerical space and time differentiations should be avoided as much as possible.

Finally, some of the results presented in this paper may be significant beyond the case of a simple straight thin-wire segment:

- For curved wires, both thin-wire integral equations derived in Section II are approximate. In that case, the choice between them is determined by their capability of handling the contribution from the current near the point of observation. There, the wire is locally straight. Hence, the reduced kernel still seems preferable.
- Explicit versions of Hallén’s equation are only available for straight wires, circular arcs, and helical wires [44]. This makes Pocklington’s equation attractive for the treatment of curved wires. In the wire-grid modeling of general structures, however, it may be feasible to use only building blocks that can be described by Hallén’s equation. The improved stability observed in Section IV may then allow more freedom in the treatment of wire junctions.
- The marching-on-in-frequency version of the CTDS approach, finally, is certainly capable of being generalized to more complicated scattering problems. In fact, this technique has already been applied successfully to a number of two-dimensional scattering problems. Its main attraction is that the error accumulation observed in marching-on-in-time computations is inherently avoided, while the computational effort does not increase.

## ACKNOWLEDGMENT

The work described in this paper was performed while the second and third authors were on leave at the Laboratory of Electromagnetic Research, Department of Electrical Engineering, Delft University of Technology, Delft, The Netherlands. The authors would like to thank the members of the Laboratory of Electromagnetic Research for creating a stimulating research atmosphere. In particular, they would like to thank Prof. H. Blok and Prof. A. T. de Hoop for stimulating discussions, and Prof. P. M. van den Berg for suggestions about the conjugate-gradient method and the role of the initial estimate. Further, the authors are indebted to Prof. R. Gómez Martín of the

Universidad de Granada, Spain, for suggesting this joint project, and to Dr. Alfonso Salinas Extremera of the same university for a useful cooperation concerning thin-wire problems. Finally, the authors would like to thank Emeritus Prof. C. J. Bouwkamp of the Technical University of Eindhoven, The Netherlands, for granting them access to his personal file on Hallén's equation.

## REFERENCES

- [1] H. C. Pocklington, "Electrical oscillations in wires," in *Proc. Camb. Phil. Soc.*, 1897, pp. 324–332.
- [2] E. Hallén, "Über die elektrischen Schwingungen in drahtförmigen Leitern," *Uppsala Universitets Årsskrift*, vol. 1, 1930 (in German).
- [3] E. Hallén, "Theoretical investigations into the transmitting and receiving qualities of antennae," *Nova Acta Regiae Societatis Scientiarum Upsaliensis*, vol. 11, series IV, 1938.
- [4] C. J. Bouwkamp, "Hallén's theory for a straight, perfectly conducting wire, used as a transmitting or receiving aerial," *Physica*, vol. 9, pp. 609–631, 1942.
- [5] R. W. P. King and D. Middleton, "The cylindrical antenna: Current and impedance," *Quart. Appl. Math.*, vol. 3, pp. 302–305, 1946.
- [6] R. W. P. King and D. Middleton, "Corrections," *Quart. Appl. Math.*, vol. 6, p. 192, 1948.
- [7] S. A. Schelkunoff, *Advanced Antenna Theory*. New York: Wiley, 1952, Section 5.3.
- [8] D. S. Jones, "Note on the integral equation for a straight wire antenna," *IEE Proc.*, vol. 128, pp. 114–116, 1980.
- [9] T. K. Sarkar, "A study of the various methods for computing electromagnetic field utilizing thin wire integral equations," *Radio Sci.*, vol. 18, pp. 29–38, 1983.
- [10] R. F. Harrington, *Field Computation by Moment Methods*. Malabar, FL: Robert E. Krieger Publishing Co., 1968, Chapter 4.
- [11] C. M. Butler, "Evaluation of potential integral at singularity of exact kernel in thin-wire calculations," *IEEE Trans. Antennas Propagat.*, vol. 23, pp. 293–296, 1975.
- [12] C. M. Butler and D. R. Wilton, "Analysis of various numerical techniques applied to thin-wire scatterers," *IEEE Trans. Antennas Propagat.*, vol. 23, pp. 534–540, 1975.
- [13] D. R. Wilton and C. M. Butler, "Efficient numerical techniques for solving Pocklington's equation and their relationships to other methods," *IEEE Trans. Antennas Propagat.*, vol. 24, pp. 83–86, 1976.
- [14] L. N. Medgyeshi-Mitschang and C. Eftimiu, "Scattering from wires and open circular cylinders of finite length using entire domain Galerkin expansions," *IEEE Trans. Antennas Propagat.*, vol. 30, pp. 628–636, 1982.
- [15] E. P. Sayre and R. F. Harrington, "Time domain radiation and scattering by thin wires," *Appl. Sci. Res.*, vol. 26, pp. 413–444, 1972.
- [16] E. K. Miller, A. J. Poggio, and G. J. Burke, "An integro-differential equation technique for the time-domain analysis of thin wire structures. 1. The numerical method," *J. Comput. Phys.*, vol. 12, pp. 24–48, 1973.
- [17] E. K. Miller, A. J. Poggio, and G. J. Burke, "An integro-differential equation technique for the time-domain analysis of thin wire structures. 2. Numerical results," *J. Comput. Phys.*, vol. 12, pp. 210–233, 1973.
- [18] E. K. Miller and J. A. Landt, "Direct time-domain techniques for transient radiation and scattering from wires," *Proc. IEEE*, vol. 68, pp. 1396–1423, 1980.
- [19] A. Rubio Bretones, R. Gómez Martín, and A. Salinas, "DOTIG1, a time-domain numerical code for the study of the interaction of electromagnetic pulses with thin-wire structures," *COMPEL*, vol. 8, pp. 39–61, 1989.
- [20] F. M. Tesche, "On the analysis of scattering and antenna problems using the singularity expansion technique," *IEEE Trans. Antennas Propagat.*, vol. 21, pp. 53–62, 1973.
- [21] K. R. Umashankar, T. H. ShumPERT, and D. R. Wilton, "Scattering by a thin wire parallel to a ground plane using the singularity expansion method," *IEEE Trans. Antennas Propagat.*, vol. 23, pp. 178–184, 1975.
- [22] M. L. van Blaricum and R. Mittra, "A technique for extracting the poles and residues of a system directly from its transient response," *IEEE Trans. Antennas Propagat.*, vol. 23, pp. 777–781, 1975.
- [23] T. K. Sarkar, "The application of the conjugate gradient method for the solution of operator equations arising in electromagnetic scattering from wire antennas," *Radio Sci.*, vol. 19, pp. 1156–1172, 1984.
- [24] S. M. Rao, T. K. Sarkar, and S. A. Dianat, "The application of the conjugate-gradient method to the solution of transient electromagnetic scattering from thin wires," *Radio Sci.*, vol. 19, pp. 1319–1326, 1984.
- [25] T. K. Sarkar, E. Arvas, and S. M. Rao, "Application of the fast Fourier transform and the conjugate gradient method for efficient solution of electromagnetic scattering from both electrically large and small conducting bodies," *Electromagnetics*, vol. 5, pp. 99–122, 1985.
- [26] S. A. Bokhari and N. Balakrishnan, "A method to extend the spectral iteration technique," *IEEE Trans. Antennas Propagat.*, vol. 34, pp. 51–57, 1986.
- [27] T. K. Sarkar, E. Arvas, and S. M. Rao, "Application of the FFT and the conjugate gradient method for the solution of electromagnetic radiation from electrically large and small conducting bodies," *IEEE Trans. Antennas Propagat.*, vol. 34, pp. 635–640, 1986.
- [28] A. T. de Hoop, "General considerations on the integral-equation formulation of diffraction problems," in *Modern Topics in Electromagnetics and Antennas*, E. J. Maanders and R. Mittra, Eds. Stevenage, UK: Peter Peregrinus, 1977, Chapter 6.
- [29] A. G. Tijhuis, "Iterative techniques for the solution of integral equations in transient electromagnetic scattering," in *PIER 5: Application of Conjugate-Gradient Methods in Electromagnetics and Signal Analysis*, T. K. Sarkar, Ed. New York: Elsevier, 1991, Chapter 13.
- [30] A. G. Tijhuis, R. Wiemans, and E. F. Kuester, "A hybrid method for solving time-domain integral equations in transient scattering," *J. Electromagnetic Waves and Appl.*, vol. 3, pp. 485–511, 1989.
- [31] C. W. Oseen, "Über die Wechselwirkung Zwischen zwei elektrischen Dipolen und über die Drehung der Polarisationssebene in Kristallen und Flüssigkeiten," *Ann. der Physik*, vol. 48, pp. 1–56, 1915 (in German).
- [32] M. Born and E. Wolf, *Principles of Optics*. Oxford: Pergamon Press, Fifth Edition, 1975, Section 2.4.2.
- [33] G. E. Albert and J. L. Synge, "The general problem of antenna radiation and the fundamental integral equation, with application to an antenna of revolution—Part I," *Quart. Appl. Math.*, vol. 6, pp. 117–131, 1948.
- [34] R. H. T. Bates, "Modal expansions for electromagnetic scattering from perfectly conducting cylinders of arbitrary cross section," *IEE Proc.*, vol. 115, pp. 1443–1445, 1969.
- [35] P. C. Waterman, "Matrix formulation of electromagnetic scattering," *Proc. IEEE*, vol. 53, pp. 805–812, 1965.
- [36] T. K. Liu and K. K. Mei, "A time-domain integral-equation solution for linear antennas and scatterers," *Radio Sci.*, vol. 8, pp. 797–804, 1973.
- [37] A. G. Tijhuis, *Electromagnetic Inverse Profiling: Theory and Numerical Implementation*. Utrecht, The Netherlands: VNU Science Press, 1987, Chapter 3.
- [38] G. H. Golub and Ch. F. Van Loan, *Matrix Computations*. Baltimore: The Johns Hopkins University Press, 1983.
- [39] P. M. van den Berg, "Iterative schemes based on the minimization of the error in field problems," *Electromagnetics*, vol. 5, pp. 237–262, 1985.
- [40] R. E. Kleinman and P. M. van den Berg, "Iterative methods for solving integral equations," in *PIER 5: Application of Conjugate-Gradient Methods in Electromagnetics and Signal Analysis*, T. K. Sarkar, Ed. New York: Elsevier, 1991, Chapter 3.
- [41] A. G. Tijhuis and Z. Q. Peng, "Marching-on-in-frequency method for solving integral equations in transient electromagnetic scattering," *IEE Proc. H*, vol. 138, pp. 347–355, 1991.
- [42] C. F. Smith, A. F. Peterson, and R. Mittra, "A conjugate gradient algorithm for the treatment of multiple incident electromagnetic fields," *IEEE Trans. Antennas Propagat.*, vol. 37, pp. 1490–1493, 1989.
- [43] D. Lesselier, D. Vuillet-Laurent, F. Jouvie, and W. Tabbara, "Iterative solution of some direct and inverse problems in electromagnetics and acoustics," *Electromagnetics*, vol. 5, pp. 147–189, 1985.
- [44] K. K. Mei, "On the integral equations of thin wire antennas," *IEEE Trans. Antennas Propagat.*, vol. 13, pp. 374–378, 1965.



**Anton G. Tijhuis (M'88)** was born in Oosterhout N.B., The Netherlands, in 1952. He received the M.Sc. degree in theoretical physics from the State University of Utrecht, the Doctor's degree from the Delft University of Technology in 1976 and 1987, respectively.

Since 1976, he has been employed at the Laboratory of Electromagnetic Research, Department of Electrical Engineering, Delft University of Technology, where he is currently an Associate Professor. During the academic year

of 1987-1988, he was a Visiting Professor at the University of Colorado at Boulder. In the summer of 1988 he was a Visiting Scientist at McDonnell-Douglas Research Laboratories, Saint Louis, Missouri, and in the summer of 1990 at the Universidad de Granada, Granada, Spain. His research interests are the analytical, numerical and physical aspects of the theory of electromagnetic waves. In particular, he has worked on transient direct-scattering problems and their application in inverse scattering.



**Peng Zhongqiu** was born in 1943 in Liaoning, China. He received the B.Sc. degree from the Harbin Engineering Institute, in 1967, and the M.Sc. and Ph.D. degrees from the Chengdu Institute of Radio Engineering, Sichuan, China, in 1981 and 1984, respectively.

From 1970 to 1979 he was employed as an Engineer at the Airborne Radar Institute, where he designed microwave components and antenna systems. In 1984, he became an Associate Professor at the Department of Electromagnetic

Field Engineering of the Chengdu Institute of Radio Engineering, Sichuan, China. From November 1989 to May 1991 he was a Visiting

Scholar with the Delft University of Technology, Delft, The Netherlands. His research involves the numerical and experimental aspects of transient antenna and scattering problems, with applications in electromagnetic remote sensing of subsurface inhomogeneities, and the calculation and measurement of RCS.



**Amelia Rubio Bretones** was born in Granada, Spain in 1961. She received the B.Sc. degree, the M.Sc. degree, and the Ph.D. degree in 1984, 1985, 1988, respectively, all in Physics and from the University of Granada, Spain.

She received a grant to work with the Electromagnetic Research Group of the Granada University during 1985. From 1985 to 1989, she was Assistant Professor, and in 1989 she was appointed Associate Professor at Granada University. During a period of three months in 1989,

she was a Visiting Scholar in the Laboratory of Electromagnetic Research, Delft University of Technology, Delft, The Netherlands. Since 1985, she has taught classes and carried out research in the area of interaction of electromagnetic waves with structures, mainly in the time domain.